

Changes in the $5d$ photoionization spectra between atomic and solid Pb

D. Iablonskyi,^{1,*} M. Patanen,^{1,2} S. Aksela,¹ and H. Aksela¹

¹*Department of Physical Sciences, University of Oulu, Box 3000, FI-90014 Oulu, Finland*

²*Synchrotron SOLEIL, l'Orme des Merisiers, Sain-Aubin, Boîte Postale 48, 91192 Gif-sur-Yvette Cedex, France*

(Received 24 April 2012; revised manuscript received 5 June 2012; published 2 July 2012)

The Pb $5d$ photoionization spectrum of free atoms and the corresponding solid state have been measured simultaneously in one experiment. In addition to the $5d$ binding-energy shifts, which were found to differ for different spin-orbit components, the lifetime of the $5d$ core hole was observed to be much shorter in solid Pb in comparison to atomic Pb. Model calculations based on a so-called excited-atom approximation were used to predict the influence of charge transfer in the observed drastic changes between atomic and solid Pb. The model indicates that level widths could serve as a sensor for a metal to nonmetal transition in neutral Pb clusters.

DOI: [10.1103/PhysRevB.86.041101](https://doi.org/10.1103/PhysRevB.86.041101)

PACS number(s): 79.60.-i, 32.80.Fb, 31.15.A-

I. INTRODUCTION

Binding-energy (BE) shifts between free atoms, molecules, and different solid compounds have been studied extensively, both experimentally and theoretically, over the years.¹⁻⁴ In only a very few experiments, however, were the BE shifts determined accurately by simultaneous measurement of the vapor and solid phases of a single element.⁵⁻⁹ In this Rapid Communication we demonstrate that simultaneous observation of both phases allows us to monitor the changes in spin-orbit splitting and lifetime broadening in addition to the BE shifts in a very demonstrative way. Based on a simple excited-atom model, the changes can be traced back to result from charge transfer towards created holes in metallic Pb.

The huge role of relativistic effects in the lead-acid battery attained notable attention recently.¹⁰ Core-hole screening was shown to serve as a probe for a metal-to-nonmetal transition in $5d$ ionized size-selected Pb_N^- ($N = 12-49$) clusters in Ref. 11. In addition, electron correlations were reported to play an important role in $5d$ photoionization of atomic Pb,¹²⁻¹⁵ creating extra structures in addition to the main $5d_{3/2}$ and $5d_{5/2}$ photoelectron lines.¹⁶ In solid Pb, the photoemission from the $5d$ level was seen to show, instead, a simple doublet structure due to spin-orbit splitting into the $5d_{3/2}$ and $5d_{5/2}$ components.¹⁷⁻²¹ Different experimental setups were used for the vapor and solid phases in previous reports, and no attention was paid to differences in linewidths.

In this work we present results of simultaneously measured Pb $5d$ photoelectron spectra from the vapor and solid phases. Accurate binding-energy shifts are obtained, and an analysis of the difference in $5d$ core-hole lifetimes between solid and atomic Pb is made. An excited-atom model using an atomic multiconfiguration Dirac-Fock (MCDHF) code is applied to explain the observations. The results provide new reference data and interesting hints for future cluster studies where the metal-to-nonmetal transition is expected to strongly influence the behavior of the $5d$ photoelectron lines.

II. EXPERIMENT

The experiments were carried out using synchrotron radiation (SR) from undulator beam line I411 at the MAX-II²² storage ring at the MAX-laboratory in Lund, Sweden. The

photoelectron spectra were measured with 55 eV photon energy. The emitted electrons were detected with a modified Scienta SES-100 electron energy analyzer²³ at the magic angle of 54.7° with respect to the polarization plane of the horizontally polarized SR, corresponding to an angularly independent atomic photoelectron spectrum. An inductively heated oven²⁴ was used to create Pb vapor condensing continuously on the Cu substrate, providing a fresh Pb surface at all times during the measurement. The electron spectrometer is computer controlled so that during a short inductive heating interval the electron signal is rejected from the detector in order to avoid disturbances from the high-frequency induction field.

For the simultaneously measured atomic and solid-state spectra, a needlelike copper wire was installed above the hole of the crucible, and the vapor was condensing on it. The position of the photon beam spot was tuned to hit the condensed solid and vapor samples. The condensed solid sample was assumed to be polycrystalline, but the layer was not studied in detail.

The experimental spectra were fitted using a Voigt profile for atomic photolines and two Doniach-Sunjic-type line shapes (corresponding to surface and bulk components) for solid photolines. A linear background was subtracted from the experimental spectra.

The $5d$ photoionization spectrum was calibrated using a BE of 25.284 eV as a reference from the photoabsorption experiment,¹² which corresponds to the atomic $5d^9(D_{5/2}^2)6s^26p_{1/2}^2$ state of Pb^+ (the highest peak in the spectrum of Fig. 1). For calibration of the valence photoionization spectrum, a BE of 7.4167 eV of $6p_{1/2}$ electron was used from the laser spectroscopic studies.²⁵

III. RESULTS AND DISCUSSION

Figure 1 shows an experimental $5d$ photoelectron spectrum taken at 55 eV photon energy simultaneously from vapor and solid Pb. For metals the core-level binding energies are lower by several eV relative to the atomic values due to the changes in the chemical environment in the initial state and the complete screening of the core hole in the photoionization process by valence electrons due to their mobility.^{2,4}

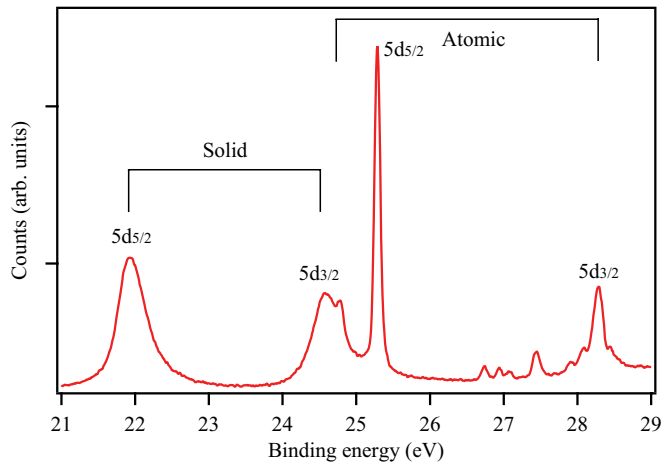


FIG. 1. (Color online) Experimental $5d$ photoelectron spectrum from the atomic and solid states of Pb taken at 55 eV photon energy.

Another unique difference between atomic and solid photoelectron peaks is the asymmetry toward the higher binding energy of the latter. This asymmetry arises mostly from the fact that electrons are losing kinetic energy (increasing binding energy) by causing excitations during their interaction with valence electrons as well as with lattice ions. Moreover, during the photoionization process surface and bulk plasmons can be excited.

The photolines from solid samples usually consist of two components corresponding to bulk and surface atoms. Usually, core-electron photolines of bulk atoms in metals appear at lower binding energies compared to the photolines of surface atoms. This is due to a more complete screening by the neighboring atoms in the final state of photoionization in the case of bulk atoms, which are more coordinated than surface atoms. In the case of solid Pb the bulk-surface shift has been recently reported to be 0.16 eV.²⁰ Results of the fitting procedure keeping the bulk-surface shift as 0.16 eV are given in Table I. The solid-state binding energies are in

TABLE I. Binding energies for $5d$ electrons in the atomic and solid states of Pb with respect to vacuum (E^V) and Fermi (E^F) levels. The energies are given in eV. The estimated experimental error bars are ± 0.01 eV for atomic lines and ± 0.05 eV for surface and bulk lines.

Sample	$E_{5d_{5/2}}^V$	$E_{5d_{5/2}}^F$	$E_{5d_{3/2}}^V$	$E_{5d_{3/2}}^F$
Atom	25.28		28.28	
Surface	22.05	18.09	24.70	20.74
		18.20 ^a		
Bulk	21.89	17.93	24.54	20.58
		18.04 ^a		
Average solid	21.93	17.97	24.58	20.62
	22.35 ^b	18.10 ^b		
	22.20 ^c		24.90 ^c	
	21.95 ^d	18.00 ^d	24.56 ^d	20.61 ^d

^aReference 20.

^bReference 11.

^cReference 26.

^dReference 21.

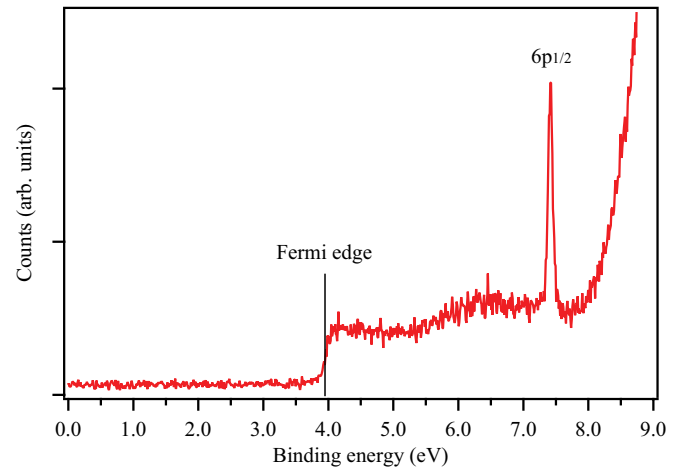


FIG. 2. (Color online) Experimental valence photoelectron spectrum of the atomic and solid states of Pb taken at 55 eV photon energy.

relatively good agreement with those determined previously within the experimental error bars.^{11,20,21} The binding-energy values from experiments on large clusters²⁶ are appreciably larger than those obtained from solid experiments.

The most striking change between atomic and solid photoelectron lines is the dramatic difference in the lifetime widths of the lines, the Lorentzian linewidths for the $5d_{5/2}$ line being 90 and 284 meV, respectively. The bulk-surface shift or the asymmetry cannot explain this difference. For example, in a previous study of K $2p$ and Rb $3d$ photoionization, atomic and solid lines were roughly of the same width.⁸ We will return to this observation after we first discuss the BE shifts of the relativistic subshells $5d_{5/2}$ and $5d_{3/2}$.

In Fig. 2 we show the outer valence region with a clear Fermi edge and a sharp atomic $6p_{1/2}$ line. We can calibrate the spectrum to vacuum level by using the known BE of the atomic $6p_{1/2}$ line.²⁵ Thus we obtain a value of 3.96 ± 0.01 eV for the Fermi edge. The solid-state binding energies can now also be obtained with reference to the vacuum level and also with reference to Fermi level by subtracting the obtained Fermi edge energy of 3.96 eV from the vacuum-referenced energies (see Table I).

Semiempirical calculations for BE shifts done by Johansson and Mårtenson⁴ combine the complete screening picture and $(Z + 1)$ approximation in the so-called Born-Haber cycle. Their BE shift value of 7.44 eV relative to the Fermi level for the $5d_{5/2}$ photoline is in good agreement with our experimental value of 7.35 eV. BE shifts of 3.1 and 3.4 eV for $5d_{5/2}$ and $5d_{3/2}$, respectively, from the investigation of large clusters ($N \sim 6500$ atoms) by Tchapyguine *et al.*²⁶ are just a bit smaller in comparison to our real atom-solid shifts, which confirms that large clusters approximate the infinite solid. All results for BE shifts are given in Table II.

An interesting observation in this work is the large difference in spin-orbit (SO) splitting between atomic and solid photolines. In the atomic case the SO splitting is 3.00 eV, while for solids it is 2.65 eV, where the atomic SO splitting is taken from the main lines assigned by $5d_{5/2}$ and $5d_{3/2}$ in Fig. 1. Such a decrease is mainly caused by the screening of the core hole and by the smaller influence of electron correlations

TABLE II. Atom-solid binding-energy shifts for the Pb 5d level. ΔE^{VV} stands for the shift where both the atomic and solid binding energies are obtained with reference to the vacuum level, and ΔE^{VF} stands for the shift where the atomic binding energy is taken with respect to vacuum level but the solid-state energy is taken with respect to Fermi level.

	$\Delta E_{5d_{5/2}}^{VV}$	$\Delta E_{5d_{5/2}}^{VF}$	$\Delta E_{5d_{3/2}}^{VV}$	$\Delta E_{5d_{3/2}}^{VF}$
This work	3.39	7.35	3.74	7.70
Large cluster (Ref. 26)	3.1		3.4	
Born-Haber cycle (Ref. 4)		7.44		

in solids. In atoms, the correlations heavily shift the main lines and redistribute the intensities between them and the satellites, as seen in Fig. 1 (for a detailed analysis of the atomic 5d photoionization spectrum see Ref. 16). The difference in passing from atoms to solids can be understood with the aid of atomic MCDF calculations. The SO splitting calculated with only two configurations $5d^9 6s^2 6p_{1/2}^2$ (which means that there are no electron correlations between valence and inner-shell electrons) is 2.82 eV. This approximation is well suited to solids because in order to account for electron correlations in the atomic case a much bigger configuration space should be used. By increasing the configuration space with all valence correlations, a calculated SO splitting of 3.03 eV approaches the experimental value for atoms. To include the screening effect in calculations we adopted the excited-atom model²⁷ and added one extra electron to the lowest unoccupied orbital; i.e., we used the configuration $5d^9 6s^2 6p_{1/2}^2 6p_{3/2}^1$. The SO splitting value calculated in this way is 2.62 eV, which is very close to the experimental value of 2.65 eV for solids. Also we were able to estimate the relativistic contribution to SO splitting, which is around 75% of total SO splitting. This is, in fact, very close to the relativistic contribution of 80% to the reaction energy for the lead battery.¹⁰

In order to explain the drastic differences in level widths we will take a look at the decay channels of the 5d hole states in atomic and solid Pb. The calculated energy-level diagram within the single configuration scheme for Pb is shown in Fig. 3. The solid phase was approximated, as was discussed before, by adding one extra electron to the $5d^{-1}$ state, i.e., with the $5d^9 6s^2 6p_{1/2}^2 6p_{3/2}^1$ configuration, and adding two extra electrons to the $6s^{-1} 6p^{-1}$ and $6p^{-2}$ states, i.e., with the $5d^{10} 6s^1 6p_{1/2}^1 6p_{3/2}^2$ and $5d^{10} 6s^2 6p_{3/2}^2$ configurations, respectively. As one can see, a new decay channel is open for solid Pb, which leads to shorter lifetimes of 5d core-hole states and in turn to wider photoelectron peaks in the spectrum of Fig. 1. To avoid having the obtained effect depend only on a particular screening electron, we used $6d_{1/2}$ and $7s$ electrons in addition to $6p_{3/2}$ in the calculations. In both cases it turned out that the $5d^{10} 6s^1 6p_{1/2}^1 nl^2$ configuration lies lower in energy than the $5d^9 6s^2 6p_{1/2}^2 nl$ configuration, where nl is $6p_{3/2}$, $6d_{1/2}$, or $7s$.

Inspection of the energy-level diagram in Fig. 3 indicates that in passing from an atomic to a solid state, the $6s^{-1} 6p^{-1}$ threshold moves across the $5d^{-1}$ threshold. This has interesting consequences: the lifetime broadening effect is expected to be seen in neutral Pb clusters where the $5d^{-1} \rightarrow 6s^{-1} 6p^{-1}$

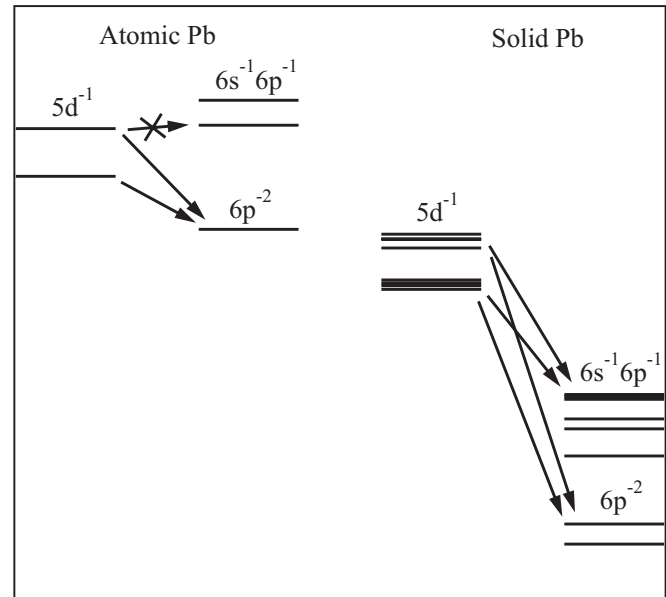


FIG. 3. Calculated energy-level diagram in the region of 5d photoionization from atomic and solid Pb. The excited-atom model is applied for solid Pb.

decay will be allowed with increasing cluster size. For given cluster sizes, the new decay channel may be open for the $5d_{3/2}^{-1}$ hole state but forbidden for the $5d_{5/2}^{-1}$ state, resulting in large differences in lifetime widths of the SO components. If the charge transfer is fully forbidden, which would most likely be the case for the nonmetallic cluster, the $5d^{-1} \rightarrow 6s^{-1} 6p^{-1}$ transition would not be energetically allowed at all according to our model calculations. Level widths would thus serve as a crucial test for the metallicity of the sample. Our prediction is based on a simple excited-atom model, which fully omits the solid-state effects, such as the formation of the 5d band. The simple model, however, explains nicely the evolution of the manyfold $5d_{3/2}$ peak structure into a single peak in passing from an atomic to a solid state and the change in the SO splitting.

In addition to the predicted lifetime broadening, the new channel is determined by the large decay amplitudes of the form $\langle 5d\epsilon l || V_{ee} || 6s6p \rangle$, which may vary as a function of the kinetic energy of the continuum orbital, making it possible for the level widths to vary with increasing cluster size. A very different behavior of the relativistic subshells is thus expected. Future experiments with neutral clusters of selected sizes would be very interesting to confirm these predictions. It should be noted that in the case of negatively charged clusters¹¹ the $5d^{-1} \rightarrow 6s^{-1} 6p^{-1}$ channel remains open independent of cluster size. There is thus an urgent need to develop a system to produce size-selected neutral Pb clusters for photoelectron experiments.

IV. CONCLUSIONS

In conclusion, in this work an experiment was carried out simultaneously for the vapor and solid phases of the Pb sample, and accurate binding-energy shifts for 5d photolines were reported. The excited-atom model was used together with

an atomic multiconfiguration Dirac-Fock code to calculate spin-orbit splitting in solid Pb, which showed the p -type screening of the $5d$ core hole. Due to charge rearrangement in solid Pb a new decay channel for the $5d$ core-hole state opens, which results in a shorter core-hole lifetime in comparison to atomic Pb. This effect is supported by our model calculations and is expected to be seen in other elements of group 14. Level widths may then serve as a sensor for the metallicity of the sample.

ACKNOWLEDGMENTS

This work has been financially supported by the Research Council for Natural Sciences and Engineering of the Academy of Finland and the European Community Research Infrastructure Action under the FP6 “Structuring the European Research Area” Programme. We thank Samuli Urpelainen, Ari Mäkinen, Terhi Kantia and also the staff of MAX-lab for their contribution during the experiments. We acknowledge Albert Djomegni and Kukwa Ernest for their help in data treatment.

*denys.iablonskyi@oulu.fi

¹D. A. Shirley, R. L. Martin, S. P. Kowalczyk, F. R. McFeely, and L. Ley, *Phys. Rev. B* **15**, 544 (1977).

²A. R. Williams and N. D. Lang, *Phys. Rev. Lett.* **40**, 954 (1978).

³J. Q. Broughton and D. L. Perry, *J. Electron Spectrosc. Relat. Phenom.* **16**, 45 (1979).

⁴B. Johansson and N. Mårtensson, *Phys. Rev. B* **21**, 4427 (1980).

⁵R. Kumpula, J. Väyrynen, T. Rantala, and S. Aksela, *J. Phys. C* **12**, L809 (1979).

⁶A. W. Potts, P. J. Brigden, D. S. Law, and E. P. F. Lee, *J. Electron Spectrosc. Relat. Phenom.* **24**, 267 (1981).

⁷S. Aksela, M. Patanen, S. Urpelainen, and H. Aksela, *New J. Phys.* **12**, 063003 (2010).

⁸M. Holappa, S. Aksela, M. Patanen, S. Urpelainen, and H. Aksela, *J. Electron Spectrosc. Relat. Phenom.* **184**, 371 (2011).

⁹S. Aksela, T. Kantia, M. Patanen, A. Mäkinen, S. Urpelainen, and H. Aksela (unpublished).

¹⁰R. Ahuja, A. Blomqvist, P. Larsson, P. Pyykkö, and P. Zaleski-Ejgierd, *Phys. Rev. Lett.* **106**, 018301 (2011).

¹¹V. Senz, T. Fischer, P. Oelßner, J. Tiggesbäumker, J. Stanzel, C. Bostedt, H. Thomas, M. Schöffler, L. Foucar, M. Martins, J. Neville, M. Neeb, Th. Möller, W. Wurth, E. Rühl, R. Dörner, H. Schmidt-Böcking, W. Eberhardt, G. Ganteför, R. Treusch, P. Radcliffe, and K.-H. Meiwes-Broer, *Phys. Rev. Lett.* **102**, 138303 (2009).

¹²J. P. Connerade, W. R. S. Garton, M. W. D. Mansfield, and M. A. P. Martin, *Proc. R. Soc. London, Ser. A* **357**, 499 (1977).

¹³S. Süzer, *J. Chem. Phys.* **72**, 6763 (1980).

¹⁴N. Sandner, V. Schmidt, W. Mehlholm, M. Y. Adam, and J. P. Desclaux, *J. Phys. B* **13**, 2937 (1980).

¹⁵H. Derenbach, H. Kossmann, R. Malutzki, and V. Schmidt, *J. Phys. B* **17**, 2781 (1984).

¹⁶S. Urpelainen, S. Heinäsmäki, M.-H. Mikkilä, M. Huttula, S. Osmekhin, H. Aksela, and S. Aksela, *Phys. Rev. A* **80**, 012502 (2009).

¹⁷G. M. Bancroft, W. Gudat, and D. E. Eastman, *Phys. Rev. B* **17**, 4499 (1978).

¹⁸J. Barth, F. Gerken, C. Kunz, V. Radojevic, M. Idrees, and W. R. Johnson, *Phys. Rev. Lett.* **55**, 2133 (1985).

¹⁹G. Le Lay, K. Hricovini, and J. E. Bonnet, *Phys. Rev. B* **39**, 3927 (1989).

²⁰J. Dalmas, H. Oughaddou, G. Le Lay, B. Aufray, G. Tréglia, C. Girardeux, J. Bernardini, J. Fujii, and G. Panaccione, *Surf. Sci.* **600**, 1227 (2006).

²¹G. M. Bancroft, W. Gudat, and D. E. Eastman, *J. Electron Spectrosc. Relat. Phenom.* **10**, 407 (1977).

²²M. Bässler, A. Ausmees, M. Jurvansuu, R. Feifel, J.-O. Forsell, P. de Tarso Fonseca, A. Kivimäki, S. Sundin, S. L. Sorensen, R. Nyholm, O. Björneholm, S. Aksela, and S. Svensson, *Nucl. Instrum. Methods Phys. Res., Sect. A* **469**, 382 (2001).

²³M. Huttula, S. Heinäsmäki, H. Aksela, E. Kukkk, and S. Aksela, *Nucl. Instrum. Methods Phys. Res., Sect. A* **467-468**, 1514 (2001).

²⁴M. Huttula, K. Jänkälä, A. Mäkinen, H. Aksela, and S. Aksela, *New J. Phys.* **10**, 013009 (2008).

²⁵J. Dembczyński, E. Stachowska, M. Wilson, P. Buch, and W. Ertmer, *Phys. Rev. A* **49**, 745 (1994).

²⁶M. Tchapyguine, S. Peredkov, A. Rosso, I. Bradeanu, G. Öhrwall, S. Legendre, S. Sorensen, N. Mårtensson, S. Svensson, and O. Björneholm, *J. Electron Spectrosc. Relat. Phenom.* **166**, 38 (2008).

²⁷D. R. Jennison, P. Weightman, P. Hannah, and M. Davies, *J. Phys. C* **17**, 3701 (1984).